PAPER

NJC
www.rsc.org/njc

2,5-Di(aryleneethynyl)pyrazine derivatives: synthesis, structural and optoelectronic properties, and light-emitting device†

Liang Zhao,[a] Igor F. Perepichka,‡[a] Figen Türksoy,[ab] Andrei S. Batsanov,[a] Andrew Beeby,[a] Karen S. Findlay[a] and Martin R. Bryce*[a]

[a] *Department of Chemistry, University of Durham, Durham, UK DH1 3LE. E-mail: m.r.bryce@durham.ac.uk; Fax: +44 191 334 2018; Tel: +44 191 384 4737*
[b] *MCTRI Polymer and Synthesis Technologies, TÜBITAK-Marmara Research Centre, P.B. 21, 41470, Gebze, Kocaeli, Turkey*

Received (in Montpellier, France) 5th February 2004, Accepted 18th March 2004
First published as an Advance Article on the web 6th July 2004

A series of 2,5-di(aryleneethynyl)pyrazine derivatives has been synthesised in 23–41% yields by two-fold reaction of 2,5-dibromo-3,6-dimethylpyrazine **3** with ethynylarenes (arene = phenyl, 2-pyridyl, 4-ethylphenyl, 4-chlorophenyl, 4-biphenyl) under standard Sonogashira conditions [CuI, $Pd(PPh_3)_2Cl_2$, NEt_3, THF]. Compound **3** has been converted into 2,5-diethynyl-3,6-dimethylpyrazine, which reacts with 2-iodothiophene to yield 2,5-bis(thien-2-ylethynyl)-3,6-dimethylpyrazine. In the X-ray crystal structure of 2,5-di(phenylethynyl)-3,6-dimethylpyrazine **4** the two phenyl rings are parallel and the pyrazine ring is inclined to their planes by 14.2°. Quantum chemical calculations establish that the HOMO–LUMO gap for **4** (3.56 eV) is lower than that of di(phenylethynyl)benzene **12** (3.72 eV). The nitrogen atoms of **4** serve to localise the HOMO on the central ring's carbon atoms, resulting in a quinoidal-type population, in contrast to **12**. Cyclic voltammetric studies establish that **4** undergoes a reduction to the radical anion at *ca.* −1.9 V (*vs.* Ag/Ag^+ in MeCN), which is almost reversible at high scan rates (500 mV s^{-1}). The UV-vis absorption and photoluminescence profiles of **4** in cyclohexane are similar to those of **12**; the emission for **4** (λ_{max} 379 and 395 nm) is red-shifted compared to **12**. Single-layer OLEDs using MEH-PPV as the emissive polymer show significantly enhanced external quantum efficiencies (up to 0.07%) when 20% by weight of 2,5-di(biphenyl-4-ethynyl)-3,6-dimethylpyrazine **8** is added as a dopant: this is ascribed to the enhanced electron-transporting properties of the pyrazine system.

Introduction

There is widespread interest in the synthesis and optoelectronic properties of new conjugated oligoarylenes containing electron-deficient heterocycles in the backbone or as pendant groups.[1] 1,3,4-Oxadiazole derivatives have been prominent in this respect[2] and it has also been established that pyridine,[3] pyrimidine,[4] quinoline[5] and 1,3,5-triazine[6] units improve electron transport characteristics compared to their phenylene analogues. This has led to their use as new materials with tailored photoluminescence and electroluminescence properties, for example as the emitting layer or as an electron-transport, hole-blocking (ETHB) layer in organic light emitting devices (OLEDs).[7] Pyrazine derivatives have been somewhat neglected in this context, although the symmetry of 2,5-disubstituted pyrazines has obvious attractions. Orange-red luminescence has been reported from thin films of polyimides containing distyrylpyrazine units in the backbone.[8] Electron injection is significantly improved in OLEDs made with a PPV–copolymer (PPV = *p*-phenylenevinylene) that contains pyrazine units in the backbone,[9] and we have shown that *p*-phenylene-2,5-dimethylpyrazine co-oligomers are efficient blue emitters in photoluminescence and electroluminescence studies.[10]

Herein we describe our work on the synthesis, structure determination and optoelectronic properties of novel 2,5-di(aryleneethynyl)pyrazines. We targeted these molecules because there is considerable current interest in the structural, optoelectronic and photophysical properties of highly conjugated oligoaryleneethynylenes.[11] For example, 1,4-bis(phenylethynyl)-benzene has been thoroughly studied[12] as a model for poly(phenyleneethynylene) derivatives that are known emitters in OLEDs.[13] Oligo(9,9-dihexyl-2,7-fluoreneethynylene)s have also been used as the emitting layer in blue OLEDs.[14] Hitherto 2,5-diethynylpyrazine units have not been studied.

Results and discussion

Synthesis

Although 2,5-dibromopyrazine is known,[15] in our hands the literature synthesis (namely, a Sandmeyer reaction on 2-amino-5-bromopyrazine)[15a] did not routinely provide sufficient material for further reactions. We, therefore, used 2,5-dibromo-3,6-dimethylpyrazine **3** as our starting reagent. An outline synthesis has been reported for this compound, although details are lacking.[16] The reaction of alanine anhydride **1** with a mixture of phosphoryl chloride and phosphorus pentachloride at 105 °C is reported to give 2,5-dichloro-3,6-dimethylpyrazine **2** in 12% yield.[17] With minor modifications to this procedure we obtained **2** in 31% yield. Conversion of compound **2** into the dibromo analogue **3** using phosphorus tribromide at 170 °C proceeded in 35% yield. In a typical reaction we obtained *ca.* 3 g of analytically pure compound **3**, and this appears to be the optimum scale for this reaction: larger-scale reactions resulted in incomplete conversion to **3**.

† Electronic supplementary information (ESI) available: tables of the optimised geometry atom coordinates; orbital contour plots for the HOMOs and LUMOs of **4** and **12**; spectra of **6**. See http://www.rsc.org/suppdata/nj/b4/b401867m/

‡ On leave from the L. M. Litvinenko Institute of Physical Organic and Coal Chemistry, National Academy of Sciences of Ukraine, R. Luxemburg Street 70, Donetsk 83114 Ukraine

DOI: 10.1039/b401867m

Two-fold Sonogashira reactions[18] on **3** using the appropriate ethynylarene derivative under standard conditions [copper iodide, triethylamine, $Pd(PPh_3)_2Cl_2$ in refluxing THF] gave products **4–8** in 23–41% yields (Scheme 1). The analogous reaction of **3** with 2-methyl-3-butyn-2-ol gave product **9**, which was deprotected under standard basic conditions[19] with loss of acetone to afford **10** (76% yield for the two steps from **3**). As an alternative route to 2,5-di(aryleneethynyl)pyrazine derivatives, we explored the Sonogashira reactions of compound **10** with iodobenzene and 2-iodothiophene. The reactions were not clean and products **4** and **11** were isolated in *ca.* 20% yields. (2-Bromothiophene gave **11** in only 10% yield). It is preferable, therefore, to use compound **3** rather than compound **10** as the pyrazine reagent in these syntheses.

X-Ray crystal structure of 4

The molecule of **4** (Fig. 1) is located at a crystallographic inversion centre. Thus, the two phenyl rings are parallel with the pyrazine ring inclined to their planes by 14.2°. Molecules in the crystal form a layer of a brickwork pattern (Fig. 1) parallel to the (0 0 1) plane. The long axes of all molecules belonging to the same layer are strictly parallel, while those in the adjacent layers are inclined to the latter by *ca.* 45°. Packing within the layer is not particularly close due to the non-planar conformation of the molecule. The separation between the mean planes of contacting molecules (3.49 Å) and the shortest intramolecular C···C distances (3.46–3.48 Å) correspond to normal Van der Waals' contacts. There is partial overlap between the phenyl ring of one molecule and the pyrazine ring of another.

Quantum chemical calculations

We performed quantum mechanical calculations of the geometry and electronic structure of compounds **4–8** and **11** by DFT methods at the B3LYP/6-31G(d) level of theory, and for compound **4** also at the B3LYP/6-311G(2d,p) level (for optimised geometries see Tables S1–S9 in the Electronic supplementary information). For reference the known phenylene analogue **12**[12] (Chart 1) was calculated at the same levels and the results of B3LYP/6-311G(2d,p) calculations for **4** and **12** were compared with X-ray diffraction single crystal structures for these compounds.[20] The calculated structures of both **4** and **12** are essentially flat and all three aromatic rings lie in the plane. There is generally a good agreement between the calculated and the X-ray experimental bond distances: mean discrepancies are 0.006 and 0.007 Å, respectively (Fig. 2). The calculated triple bond lengths are somewhat longer (by 0.003–0.008 Å) and the single bonds (between the aromatic rings and sp-hybrid carbon atoms) are somewhat shorter (by 0.008–0.012 Å) than the experimental data, but these are expected differences because the calculated values are inter-nuclear distances whereas X-ray gives interatomic distances based on mean electronic density, which for the fragment ≡C– is shifted towards the triple bond.

Orbital energy level analysis for compounds **4–8**, **11** and **12** at the B3LYP/6-31G(d) level is summarised in Table 1, indicating that all pyrazine derivatives are stronger electron acceptors than compound **12** (their LUMO energies are lower than that in **12** by 0.26–0.60 eV). Although their HOMO energy levels are higher than that in **12**, in total all pyrazine derivatives show a narrower HOMO–LUMO gap as compared to **12**.

Calculations performed for compounds **4** and **12** at the higher B3LYP/6-311G(2d,p) level for more precise estimation of orbital energies showed *ca.* 0.21–0.26 eV lower energies as compared to B3LYP/6-31G(d) calculations, although the general trend remains the same and HOMO–LUMO gap energies calculated by both methods are very close (3.53 and 3.56 eV for **4**, 3.70 and 3.72 eV for **12**, respectively). For pyrazine

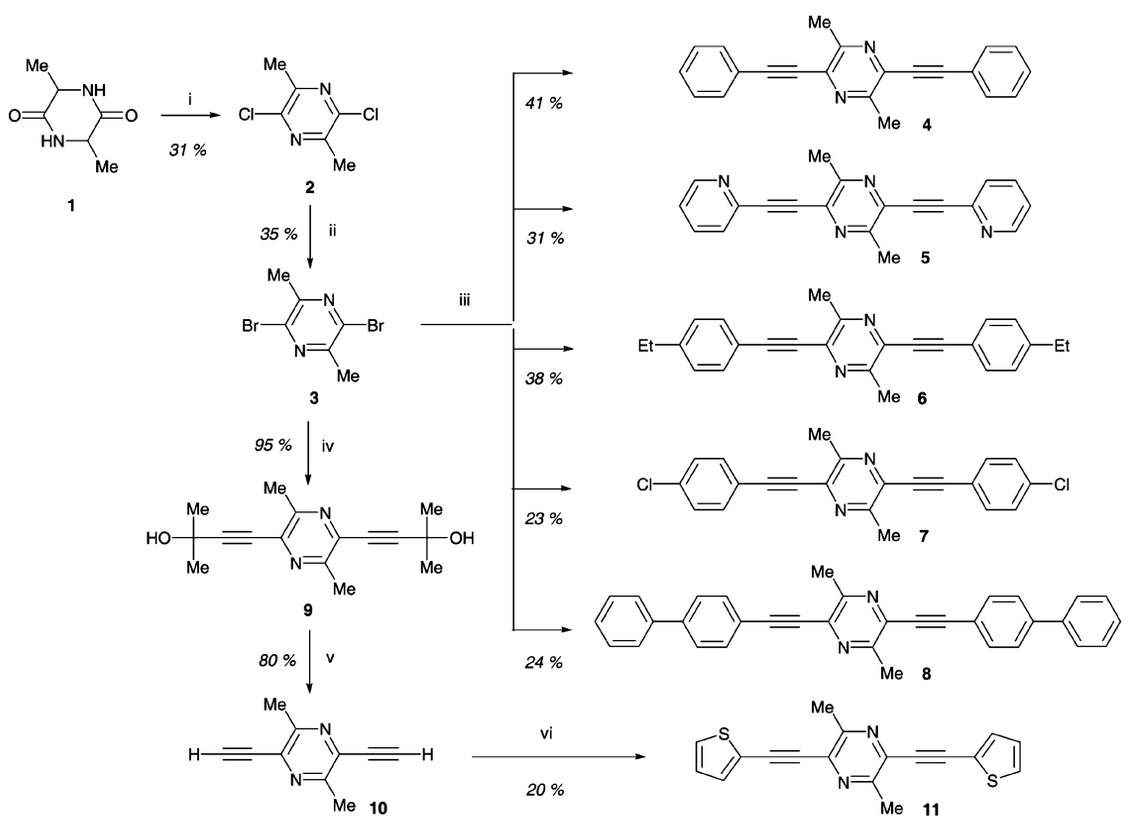

Scheme 1 Synthesis of 2,5-(diaryleneethynyl)pyrazines. *Reagents and conditions*: (i) $POCl_3/PCl_5$, 105 °C, 24 h; (ii) PBr_3, 170 °C, 24 h; (iii) ArC≡CH, CuI, Et_3N, $Pd(PPh_3)_2Cl_2$, THF, 20 °C/1 h, 65 °C/1.5 h; (iv) $Me_2C(OH)$–C≡CH, CuI, Et_3N, THF, 20 °C, 1 h, reflux; (v) NaOH, toluene, reflux; (vi) 2-iodothiophene, CuI, Et_3N, $Pd(PPh_3)_2Cl_2$, THF, 20 °C/1 h, 65 °C/1.5 h.

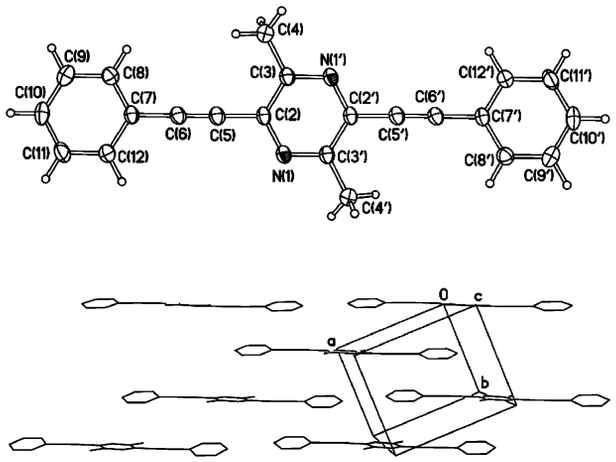

Fig. 1 (top) Molecular structure of **4**. Thermal ellipsoids are drawn at 50% probability level. Atoms generated by the inversion centre are primed. (bottom) Layer of molecules in the crystal structure; projection on the (0 0 1) plane.

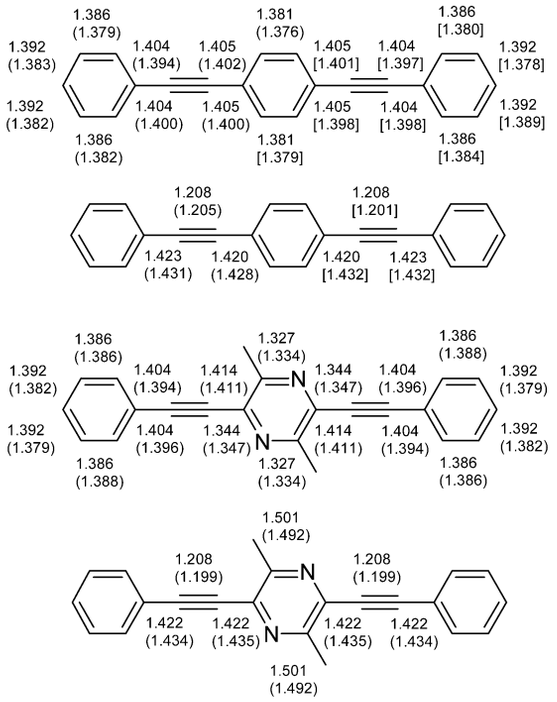

Fig. 2 B3LYP/6-311G(2d,p) calculated bond distances in phenylene **12** and dimethylpyrazine **4** derivatives. Bond distances from X-ray analysis are given in parentheses for comparison (distances for the two independent molecules from the X-ray crystal structure of phenylene derivative **12** are given in parentheses and square brackets, respectively). The structures at the top show bond distances in the rings and while those at the bottom show acyclic bond distances.

derivative **4** (as compared to **12**) the energies of both HOMO and LUMO orbitals decrease (by 0.17 and 0.33 eV, respectively) with, as expected, more pronounced changes in the LUMO energy due to the electronegative nitrogen atoms (Fig. 3). As a result the HOMO–LUMO gap contracts by 0.16 eV, from 3.72 eV for **12** to 3.56 eV for **4**. For compound **12** the HOMO is located on the C–C triple bonds as well as on the central 1,4-phenylene ring, with only minor population on the outer phenyl moieties. The main population at the central ring is on C–1 and C–4, which form bonding orbitals with adjacent carbons. In **4**, the HOMO is also located on the triple C–C bonds and on the central ring. The electronegative nitrogen atoms in **4** result in localisation of the HOMO on the central ring's carbon atoms, giving a quinoidal-type population, in contrast to **12**. The LUMO in **12** populates the exocyclic C–C single bond and C–2,3, C–5,6 bonds of the central phenylene ring, resulting in a quinoidal structure. Similar localisation of the LUMO on the exocyclic C–C single bonds is observed for **4**, whereas for the pyrazine ring the LUMO is localised on the nitrogen atoms (Fig. 4).

The population of the unoccupied molecular orbitals LUMO + 1 to LUMO + 4 is similar for both molecules **4** and **12** (Fig. S1 in ESI): LUMO + 1 is shifted to the outer phenyl rings, which become essentially quinoidal; LUMO + 2 is localised on the central ring, forming antibonding orbitals between C2–C3, C5–C6 and N1–C6, C3–N4 for **12** and **4**, respectively. Structures LUMO + 3 and LUMO + 4 for both compounds are nearly the same, with population on the terminal phenyl rings. For occupied HOMO − 1 to HOMO − 4 orbitals, the structures of HOMO − 1 and HOMO − 3 orbitals for both compounds are quite similar, whereas a large difference is observed for HOMO − 2, which is quinoidally localised on the end phenyls in **12** and on the central pyrazine ring in **4**, involving participation of methyl groups and the nitrogen lone pairs.

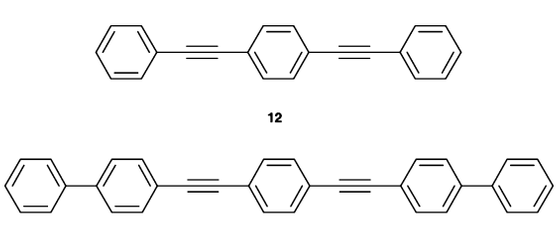

12

13

Chart 1

Solution electrochemical properties

The redox properties of compound **4**, studied by cyclic voltammetry (CV) in dry deoxygenated acetonitrile solution, show an irreversible oxidation to the radical cation at +1.62 V *vs.* Ag/Ag^+ (Fig. 5). Reduction of **4** to its radical anion occurs at quite high negative potentials of *ca.* −1.87 V (*vs.* Ag/Ag^+). At slow scan rates (20–50 mV s^{-1}) the reduction is an irreversible process (not shown on Fig. 5). On increasing the scan rate to 100 mV s^{-1} it becomes partly reversible ($i_c \gg i_a$) and, remarkably, at a high scan rate of 500 mV s^{-1} the process is almost reversible ($i_c \approx i_a$; $\Delta E_{pa-pc} = 77$ mV). The electrochemical band gap, estimated from the oxidation and reduction onsets (+1.45 V and −1.78 V) is $E_g^{CV} = 3.23$ eV, which is in reasonable agreement with the optical band gap estimated from the red edge of the longest wavelength absorption ($\lambda = 382$ nm, $E_g^{opt} = 3.25$ eV) and close to the calculated value of the HOMO–LUMO gap (3.56 eV). No clear reduction peak was observed in the CV of compound **12** within the acetonitrile solvent window, under the same experimental conditions, demonstrating the enhanced electron-accepting ability of compound **4**, due to the presence of the pyrazine ring.

Table 1 HOMO/LUMO energy levels for compounds **4**–**8**, **11** and **12** from B3LYP/6-31G(d) calculations

Compound	HOMO/eV	LUMO/eV	$\Delta E_{HOMO-LUMO}$/eV
4	−5.62	−2.09	3.53
5	−5.86	−2.30	3.56
6	−5.48	−2.00	3.48
7	−5.81	−2.34	3.47
8	−5.48	−2.15	3.33
11	−5.47	−2.20	3.27
12	−5.43	−1.74	3.70

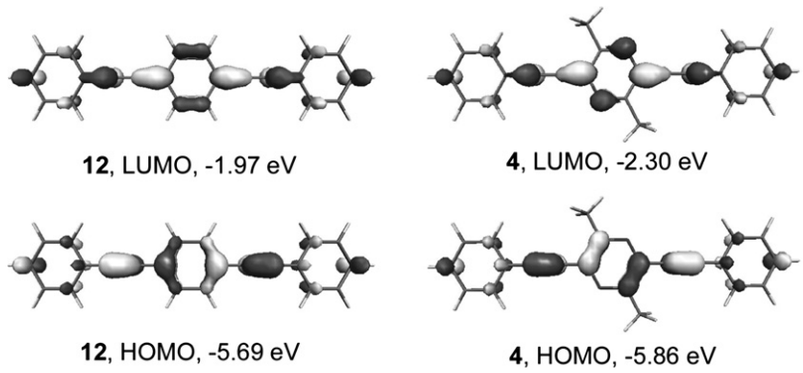

Fig. 3 Frontier orbitals of compounds **12** and **4** calculated by B3LYP/6-311G(2d,p) DFT method.

Absorption and photoluminescence studies on 4 and 6

The absorption and steady state fluorescence spectra in cyclohexane were recorded at ambient temperature for compounds **4** and **6** (Fig. 6 and S2 in ESI). The major absorption, emission and excitation maxima are given in Table 2, along with data for compound **12**.[12] The absorbances of these compounds were recorded between 230 and 400 nm and are characterised by two broad bands, with the longer wavelength bands at λ_{max} 354 and 359 nm for **4** and **6**, respectively, showing a similar profile to that observed for **12** at ambient temperature. It is believed that these spectral profiles represent the time-averaged spectra of the various rotamers present at these temperatures.[12]

The emission spectra of **4** and **6** were independent of excitation wavelength. The fluorescence profiles and the excitation spectra coincide well with the corresponding absorption spectra. There is a small Stokes shift between the excitation and emission spectra. The emission spectra have some vibrational fine structure and resemble that of **12**, although the maxima for **4** and **6** are red-shifted compared to **12**. The difference in the excitation and emission profiles is attributed to differences in the geometric arrangement of the nuclei in the ground and excited states, resulting from the low barrier to rotation about the alkynyl–aryl single bond.[11b,12] The vibrational structure in the emission spectra is indicative of an S_1 state with a larger barrier to rotation from the lowest energy planar orientation of the rings. The ethyl substituents in **6** only slightly lower the S_1 excited state.

Electroluminescent device studies

The potential of 2,5-di(aryleneethynyl)pyrazine derivatives **4**, **5** and **8** to act as electron-transport materials in OLEDs has been explored by blending the compound as a dopant into thin films of poly[2-(2-ethylhexyloxy)-5-methoxy-1,4-phenylenevinylene] (MEH-PPV), following the precedent set by Heeger's group.[21] Analogous experiments using the phenylene analogues **12** and **13** (Chart 1) were performed for comparison. Preliminary data establish that the electroluminescence (EL) characteristics of single-layer devices in the configuration ITO/MEH-PPV + dopant/Al were unchanged compared to an MEH-PPV reference device (*i.e.*, no added dopant) by addition of compounds **4**, **5**, **12** and **13**. On the other hand, using compound **8** as the dopant led to a marked increase in the external quantum efficiency of the device (0.07% at a current density of 10 mA cm^{-3}) compared to the reference device (*ca.* 2×10^{-3}%) although more rapid deterioration in the EL output was observed for the MEH-PPV + **8** layers. The EL spectra of all the device structures are very similar, which suggests that, as expected, emission is due to the MEH-PPV polymer [λ_{max}^{EL} = 575, 640 (sh) nm]. The non-planar biphenyl units of **8** probably serve to reduce crystallisation (and hence segregation) of the dopant in the blend. A comparison between **8** and **13** demonstrates the benefit of the electron-deficient pyrazine unit. We have previously reported similar levels of enhancement of the external quantum efficiencies of MEH-PPV devices doped with oxadiazole-pyridine hybrid compounds as the electron-transport material.[22] Further studies on single blended-layer OLEDs will be published shortly.

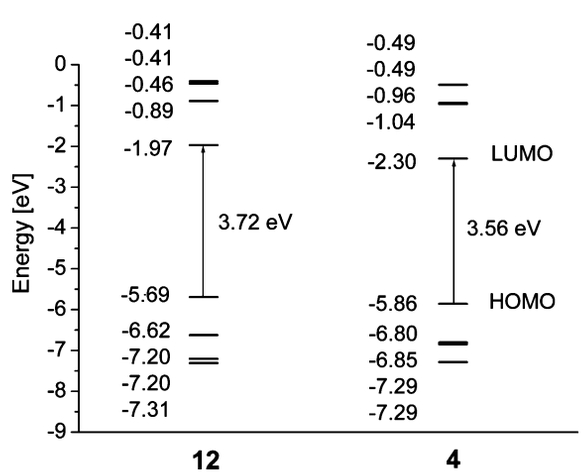

Fig. 4 B3LYP/6-311G(2d,p) orbital energy level diagrams for phenylene **12** and dimethylpyrazine **4** derivatives.

Conclusions

2,5-Di(aryleneethynyl)pyrazine derivatives have been studied for the first time. In particular, the structural, electrochemical

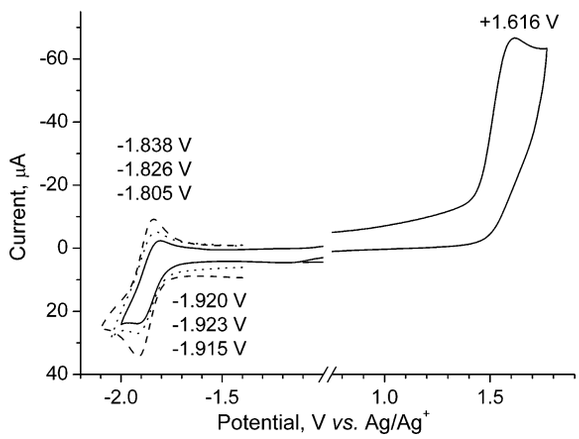

Fig. 5 Cyclic voltammogram for derivative **4** in acetonitrile/0.1 M Bu_4NPF_6 (20 °C) at different scan rates: (—) 100 mV s^{-1} ($E_{red}^{1/2}$ = −1.863 V; $\Delta E_{pa\text{-}pc}$ = 115 mV); (···) 200 mV s^{-1} ($E_{red}^{1/2}$ = −1.874 V; $\Delta E_{pa\text{-}pc}$ = 97 mV); (---) 500 mV s^{-1} ($E_{red}^{1/2}$ = −1.876 V; $\Delta E_{pa\text{–}pc}$ = 77 mV).

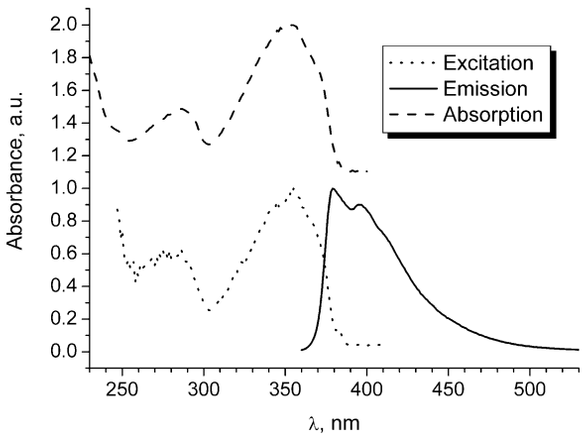

Fig. 6 Normalised absorbance, excitation (for 432 nm emission wavelength) and emission (for 354 nm excitation wavelength) spectra of compound **4** in cyclohexane.

and photophysical properties of derivative **4** have been compared with those of di(phenylethynyl)benzene **12**. The presence of the pyrazine ring leads to a significant enhancement of electron-accepting properties, as revealed by cyclic voltammetric data. Quantum chemical calculations confirm these observations. Preliminary experiments establish the potential for diethynylpyrazine derivative **8** to act as an electron-transporting material as a blend with MEH-PPV in single-layer OLEDs. The compounds reported herein are attractive for photophysical studies and compound **10** should be a very useful and versatile building block for the synthesis of new, more highly functionalised pyrazine derivatives, including conjugated oligomers for optoelectronic device applications.

Experimental

General

^{1}H NMR spectra were recorded on Varian VXR 400s and Varian Inova 500 instruments, operating at 400 and 500 MHz, respectively. Chemical shifts are quoted in ppm, relative to tetramethylsilane (TMS), using TMS or the residual solvent as internal reference. ^{13}C NMR spectra were recorded using broad band decoupling, on the Varian VXR 400s or Varian Inova 500 at 100 MHz and 125 MHz, respectively. Electron impact (EI) mass spectra were recorded on a Micromass AutoSpec spectrometer operating at 70 eV with the ionisation mode as indicated. An Ati Unicam UV/VIS UV2 spectrometer was used to record the absorption spectra of the samples, which were held in 1 cm path length cuvettes. Emission and excitation spectra were recorded using a Jobin–Yvon Horiba Fluorolog 3-22 Tau-3 spectrofluorimeter. The spectra of dilute solutions with absorbance of less than 0.1 in the 200 to 400 nm range were recorded using conventional 90 degree geometry.

Table 2 The absorption and steady state emission and excitation spectra of **4**, **6** and **12**[a]

Compound	λ_{abs}/nm	λ_{PL}/nm	λ_{ex}/nm
4	286 (br), 354 (br)	379, 395 (br)	283 (br), 357 (br)
6	291, 359 (br), 376 (sh)	384, 403, 418	287, 360, 374 (sh)
12	320, 345 (sh)	346, 362, 375	319, 340 (sh)

[a] br – broad, sh – shoulder.

Device fabrication

For OLED studies a mixed solution containing MEH-PPV and 20% by weight of the dopant was prepared using *p*-xylene and chloroform as solvents (1:1 v/v) and films of *ca.* 100 nm thickness were produced by spin-coating. ITO-coated glass was used as the anode, and an Al top electrode was evaporated onto the organic film.

X-Ray crystallography

The experiment was carried out on a Bruker 3-circle diffractometer with a SMART 6K CCD area detector, using graphite-monochromated Mo-K_α radiation ($\bar{\lambda} = 0.71073$ Å). The crystal was maintained at low temperature ($T = 120$ K), using a Cryostream (Oxford Cryosystems) open-flow N_2 cryostat. The structure was solved by direct methods and refined by full-matrix least squares against F^2 of all data, using SHELXTL software. Compound **4** crystal data: $C_{22}H_{16}N_2$, MW = 308.37, monoclinic, space group $P2_1/c$ (No. 14), $a = 9.059(1)$, $b = 7.515(1)$, $c = 12.102(4)$ Å, $\beta = 92.33(1)°$, $U = 823.2(3)$ Å^3, $Z = 2$, $D_c = 1.244$ g cm^{-3}, $\mu = 0.07$ mm^{-1}. Full sphere of reciprocal space was covered by four sets of 0.3° ω scans, each set with different φ and/or 2θ angles, yielding 10,887 reflections with $2\theta \leq 55°$, of which 1891 were independent ($R_{int} = 0.039$). All non-hydrogen atoms were refined in anisotropic approximation; all H atoms were located in a difference Fourier map and refined in isotropic approximation. The refinement of 240 parameters converged at $R = 0.038$ [for 1465 reflections with $F^2 \geq \sigma(F^2)$] and $wR(F^2) = 0.115$ (for all data).§

Electrochemistry

Cyclic voltammetry experiments were performed on a BAS CV50W electrochemical analyser with *iR* compensation. Platinum wire, platinum disk (ø 1.6 mm) and Ag/Ag$^+$ (0.01 $AgNO_3$ in acetonitrile) were used as counter, working, and reference electrodes, respectively. CV experiments were performed in dry acetonitrile with 0.1 M Bu_4NPF_6 as supporting electrolyte. The scan rate was varied from 50 to 2000 mV s^{-1}. The potentials were referred to the Fc/Fc$^+$ couple as the internal reference, which showed a potential of +0.08 V *vs.* Ag/Ag$^+$ in our conditions.

Computational procedures

The *ab initio* computations of compounds **4**–**9** and **12** were carried out with the Gaussian 98[23] package of programs at the density functional theory (DFT) level using Pople's 6-31G and 6-311G split valence basis sets supplemented by one or two d-functions on heavy atoms and p-polarisation functions on hydrogens (or without them). DFT calculations were carried out using Becke's three-parameter hybrid exchange functional[24] with Lee–Yang–Parr gradient-corrected correlation functional (B3LYP).[25] Thus, the geometries were optimised with B3LYP/6-31G(d) and for compounds **4** and **12** also with B3LYP/6-311G(2d,p); electronic structures were calculated at the same level. Contours of the five highest occupied and five lowest unoccupied molecular orbitals were visualised using the Molekel v.4.2 program.[26] No constraints to bonds/angles/dihedral angles were applied in the calculations and all the atoms were free to optimise.

§ CCDC reference number 231332. See http://www.rsc.org/suppdata/nj/b4/b401867m/ for crystallographic data in .cif or other electronic format.

Syntheses

2,5-Dichloro-3,6-dimethylpyrazine 2. To alanine anhydride **1** (25.0 g, 0.176 mol) in $POCl_3$ (150 cm^3), PCl_5 (9.0 g) was added and the mixture was heated (oil bath temperature 105 °C) for 24 h. The mixture was cooled to room temperature and excess $POCl_3$ was removed by vacuum distillation. Cold brine was added slowly with stirring and a white solid formed after standing for 12 h. Then the mixture was extracted with dichloromethane and the organic layer was dried with $MgSO_4$. The solvent was removed by vacuum evaporation and the residue was chromatographed on silica eluted with dichloromethane, followed by crystallisation from hexane to yield compound **2** as a white solid (9.3 g, 31%), m.p. 73–74 °C (lit.[17] m.p. 72 °C). Found C, 40.12; H, 3.78; N, 15.63%. $C_6H_6Cl_2N_2$ requires C, 40.71; H, 3.42; N, 15.82%. MS (EI): m/z 176 (M^+, 100%). ^{1}H NMR ($CDCl_3$): δ 2.61 (6H, s, CH_3). ^{13}C NMR ($CDCl_3$): δ 21.24, 145.60, 149.77.

2,5-Dibromo-3,6-dimethylpyrazine 3. A mixture of **2** (5.37 g 30 mmol) and PBr_3 (15 cm^3) was stirred at reflux (oil bath temperature 170 °C) for 24 h then cooled to 20 °C and excess PBr_3 removed by vacuum distillation. Work up and purification as described for **2** gave compound **3** (2.8 g, 35%) as a white solid, m.p. 84.4–85.8 °C. Found C, 26.76; H, 2.52; N, 10.35%. $C_6H_6Br_2N_2$ requires C, 27.10; H, 2.27; N, 10.53%. MS (EI): m/z 266 (M^+ 100%). ^{1}H NMR ($CDCl_3$): δ 2.58 (6H, s, CH_3). ^{13}C NMR ($CDCl_3$): δ 22.97, 138.80, 152.4.

Preparation of 4-8: general procedure. To the solution of 2,5-dibromo-3,6-dimethylpyrazine **3** (0.51 g, 2.0 mmol) and the alkynylarene (4.8 mmol) in dry THF (7.0 cm^3), CuI powder (10.6 mg) was added. Triethylamine (0.9 cm^3) was added and the solution was stirred at 20 °C for 10 min to obtain a clear solution. $Pd(PPh_3)_2Cl_2$ (32 mg) was added in one portion and the mixture was stirred at 20 °C for 1 h, followed by reflux at 65 °C for another 1.5 h. The mixture was cooled to room temperature and the solid that formed during the reaction was removed by vacuum filtration. The filtrate was chromatographed on silica, eluted with DCM, followed by crystallisation from hexane. The compounds were thereby obtained as yellow solids.

2,5-Dimethyl-3,6-bis(phenylethynyl)pyrazine **4**. 41% yield, m.p. 169–170 °C. Found: C, 85.44; H, 5.21; N, 9.15%. $C_{22}H_{16}N_2$ requires C, 85.69; H, 5.23; N, 9.08%. MS (EI): m/z 308, (M^+, 100%). ^{1}H NMR ($CDCl_3$): δ 2.69 (6H, s, CH_3) 7.32 (6H, s, CH) 7.58 (4H, s, CH). ^{13}C NMR ($CDCl_3$): δ 21.75, 86.45, 96.72, 121.85, 128.51, 129.49, 132.06, 136.24, 153.02.

2,5-Dimethyl-3,6-bis(pyridin-2-ylethynyl)pyrazine **5**. 31% yield, m.p. 201–202 °C. Found: C, 77.24; H, 4.57; N, 17.89%. $C_{20}H_{14}N_4$ requires C, 77.40; H, 4.55; N, 18.05%. MS (EI): m/z 310 (M^+, 100%). ^{1}H NMR ($CDCl_3$): δ 2.60 (6H, s, CH_3), 7.31 (2H, s, CH), 7.48 (2H, s, CH), 8.56 (2H, s, CH). ^{13}C NMR ($CDCl_3$): δ 20.13, 72.46, 123.31, 127.26, 135.34, 137.42, 149.41, 153.97.

2,5-Bis(4-ethylphenylethynyl)-3,6-dimethylpyrazine **6**. 38% yield, m.p. 196.5–198.3 °C. MS (EI): m/z 364, (M^+, 100%). HRMS (EI): (M^+) calcd. for $C_{26}H_{24}N_2$ 364.19395; found 364.19400. ^{1}H NMR ($CDCl_3$): δ 1.19 (6H, t, $J = 7.6$ Hz, CH_3), 2.62 (4H, q, $J = 7.6$ Hz, CH_2), 2.68 (6H, s, CH_3), 7.15 (4H, d, $J = 8$ Hz, CH), 7.48 (4H, d, $J = 8$ Hz, CH). ^{13}C NMR ($CDCl_3$): δ 15.89, 22.15, 29.78, 86.20, 97.81, 119.73, 128.22, 132.31, 136.23, 148.34, 152.68.

2,5-Bis(4-chlorophenylethynyl)-3,6-dimethylpyrazine **7**. 23% yield, m.p. 190.5–191 °C. MS (EI): m/z 376 (M^+, 58%), 270 (100%). HRMS (EI): (M^+) calcd. for $C_{22}H_{14}Cl_2N_2$ 376.05340; found 376.05329. ^{1}H NMR ($CDCl_3$): δ 2.69 (6H, s, CH_3), 7.31 (4H, s, CH), 7.48 (4H, s, CH). ^{13}C NMR ($CDCl_3$): δ 20.93, 74.66, 81.84, 120.63, 127.20, 133.21, 141.56, 156.45.

2,5-Bis(biphenyl-4-ylethynyl)-3,6-dimethylpyrazine **8**. 24% yield, m.p. 188.0–188.7 °C. MS (EI): m/z 460, (M^+ 100%). HRMS (EI): (M^+) calcd. for $C_{34}H_{24}N_2$ 460.19395; found 460.19385. ^{1}H NMR ($CDCl_3$): δ 2.62 (6H, s, CH_3), 7.18 (2H, s, CH), 7.29 (4H, s, CH), 7.38 (8H, s, CH), 7.61 (4H, s, CH). ^{13}C NMR ($CDCl_3$): δ 14.68, 74.66, 81.84, 120.63, 127.07, 127.14, 127.88, 128.93, 132.97, 140.10, 141.97, 156.91.

4-[5-(3-Hydroxy-3-methyl-but-1-ynyl)-3,6-dimethylpyrazin-2-yl]-2-methylbut-3-yn-2-ol 9. Compound **3** (810 mg, 3.04 mmol), 2-methylbut-3-yn-2-ol (1.54 g, 18.24 mmol), CuI (58 mg), $Pd(PPh_3)_2Cl_2$ (213 mg) and triethylamine (10 cm^3) were mixed in dry THF (15 cm^3) and stirred at room temperature for 1 h, then at reflux under Ar to obtain a brownish suspension. The mixture was filtered and the precipitate was washed with diethyl ether. The filtrate was evaporated under reduced pressure. The residue was purified by column chromatography on silica [eluent: ethyl acetate–petroleum ether (b.p. 40–60 °C), 7:3 (v/v)] to give compound **9** as white solid (780 mg, 95%), m.p. 170–171 °C. Found: C, 70.43; H, 7.67; N, 10.02%. $C_{16}H_{20}N_2O_2$ requires C, 70.56; H, 7.40; N, 10.29%. MS (EI): m/z 272 (M^+, 100%). ^{1}H NMR ($CDCl_3$): δ 1.59 (12H, s, CH_3), 2.10 (2H, s, OH), 2.55 (6H, s, CH_3). ^{13}C NMR ($CDCl_3$): δ 21.77, 31.34, 65.85, 79.40, 101.48, 136.18, 153.10.

2,5-Diethynyl-3,6-dimethylpyrazine 10. Compound **9** (200 mg, 0.735 mmol) was dissolved in dry toluene (15 cm^3). Sodium hydroxide powder (freshly ground from pellets; 64 mg) was added and the mixture was refluxed under Ar until **9** was completely consumed (TLC monitoring). The mixture was cooled to room temperature then suction filtered through a celite pad. The filtrate was evaporated *in vacuo* and residue was purified by column chromatography on silica [eluent: ethyl acetate–petroleum ether (b.p. 40–60 °C), 5:4 (v/v)] to give compound **10** as a pale-yellow solid (88 mg, 80%), m.p. 175–176 °C. Found: C, 76.67; H, 5.34; N, 17.74%. $C_{10}H_8N_2$ requires C, 76.90; H, 5.16; N, 17.94%. MS (EI): m/z 156 (M^+, 100%). ^{1}H NMR ($CDCl_3$): δ 2.59 (6H, s, CH_3), 3.48 (2H, s, CH). ^{13}C NMR ($CDCl_3$): δ 21.92, 80.32, 85.74, 136.08, 153.64.

2,5-Bis(thien-2-ylethynyl)-3,6-dimethylpyrazine 11. Compound **10** (200 mg, 1.28 mmol), 2-iodothiophene (1.08 mg, 5.12 mmol), CuI (24 mg), $Pd(PPh_3)_2Cl_2$ (89 mg) and triethylamine (10 cm^3) were mixed in dry THF (15 cm^3) and reacted according to the general procedure above. Column chromatography [silica, dichloromethane–hexane, 1:1 (v/v)] gave compound **11** as a yellow solid (81 mg, 20% yield), m.p. 145–147 °C (dec). MS (EI): m/z 319.98 (M^+, 100%). HRMS (EI): (M^+) calcd. $C_{18}H_{12}N_2S_2$ 320.0450; found 320.0441. ^{1}H NMR ($CDCl_3$): δ 7.36 (2H, d, $J = 4.8$ Hz), 7.34 (2H, d, $J = 6.4$ Hz), 6.99 (2H, t, $J = 8.8$ Hz), 2.61 (6H, s). ^{13}C NMR ($CDCl_3$): δ 22.17, 90.47, 110.00, 121.91, 127.66, 129.48, 134.10, 136.21, 153.04.

Compounds **12** and **13** were obtained analytically pure using standard procedures.[12]

Acknowledgements

We thank the Royal Society and the Royal Society of Chemistry Journals Grant for International Authors for funding visits to Durham (I.F.P.), and One North-East *via* the County Durham Sub-regional Partnership project SP/082 for funding the purchase of equipment used in this work.

References

1 M. Thelakkat and H.-W. Schmidt, *Polym. Adv. Technol.*, 1998, **9**, 429.

2 (*a*) K. Chondroudis and D. B. Mitzi, *Chem. Mater.*, 1999, **11**, 3028; (*b*) C. Wang, M. Kilitziraki, L.-O. Palsson, M. R. Bryce, A. P. Monkman and I. D. W. Samuel, *Adv. Funct. Mater.*, 2001, **11**, 47; (*c*) C. Wang, G.-Y. Jung, A. S. Batsanov, M. R. Bryce and M. C. Petty, *J. Mater. Chem.*, 2002, **12**, 173; (*d*) Y.-Y. Chien, K.-T. Wong, P.-T. Chou and Y.-M. Cheng, *Chem. Commun.*, 2002, 2874; (*e*) J. H. Kim, J. H. Park and H. Lee, *Chem. Mater.*, 2003, **15**, 3414.

3 (*a*) J. A. Irvin, C. J. DuBois and J. R. Reynolds, *Chem. Commun.*, 1999, 2121; (*b*) S.-C. Ng, H.-F. Lu, H. S. O. Chan, A. Fujii, T. Laga and K. Yoshino, *Adv. Mater.*, 2000, **12**, 1122; (*c*) C. Wang, M. Kilitziraki, J. A. H. MacBride, M. R. Bryce, L. Horsburgh, A. Sheridan, A. P. Monkman and I. D. W. Samuel, *Adv. Mater.*, 2000, **12**, 217; (*d*) A. P. Monkman, L.-O. Palsson, R. W. T. Higgins, C. Wang, M. R. Bryce and J. A. K. Howard, *J. Am. Chem. Soc.*, 2002, **124**, 6049.

4 (*a*) K.-T. Wong, T. S. Hung, Y. Lin, C.-C. Wu, G.-H. Lee, S.-M. Peng, C. H. Chou and Y. O. Su, *Org. Lett.*, 2002, **4**, 513; (*b*) C. C. Wu, Y. T. Lin, H. H. Chiang, T. Y. Cho, C. W. Chen, K. T. Wong, Y. L. Liao, G. H. Lee and S. M. Peng, *Appl. Phys. Lett.*, 2002, **81**, 577; (*c*) G. Hughes, C. Wang, A. S. Batsanov, M. Fearn, S. Frank, M. R. Bryce, I. F. Perepichka, A. P. Monkman and B. P. Lyons, *Org. Biomol. Chem.*, 2003, **1**, 3069.

5 X. Zhang and S. A. Jenekhe, *Macromolecules*, 2000, **33**, 2069.

6 (*a*) J. M. Lupton, L. R. Hemingway, I. D. W. Samuel and P. L. Burn, *J. Mater. Chem.*, 2000, **10**, 867; (*b*) J. Pang, Y. Tao, S. Freiberg, X.-P. Yang, M. D'Iorio and S. Wang, *J. Mater. Chem.*, 2002, **12**, 206.

7 (*a*) Reviews: A. Kraft, A. C. Grimsdale and A. B. Holmes, *Angew. Chem., Int. Ed.*, 1998, **37**, 402; (*b*) Y. Shirota, *J. Mater. Chem.*, 2000, **10**, 1; (*c*) U. Mitschke and P. Bäuerle, *J. Mater. Chem.*, 2000, **10**, 1471.

8 A. Wu, T. Akagi, M. Jikei, M. Kakimoto, Y. Imai, S. Ukishima and Y. Takahashi, *Thin Solid Films*, 1996, **273**, 214.

9 Z. Peng and M. E. Galvin, *Chem. Mater.*, 1998, **10**, 1785.

10 F. Türksoy, G. Hughes, A. S. Batsanov and M. R. Bryce, *J. Mater. Chem.*, 2003, **13**, 1554.

11 (*a*) U. H. F. Bunz, *Chem. Rev.*, 2000, **100**, 1605; (*b*) M. I. Sluch, A. Godt, U. H. F. Bunz and M. A. Berg, *J. Am. Chem. Soc.*, 2001, **123**, 6447.

12 A. Beeby, K. Findlay, P. J. Low and T. B. Marder, *J. Am. Chem. Soc.*, 2002, **124**, 8280 and references therein.

13 (*a*) A. Montali, P. Smith and C. Weder, *Synth. Met.*, 1998, **97**, 123; (*b*) C. Schmitz, P. Pösh, M. Thelakkat, H.-W. Schmidt, A. Montali, K. Feldman, P. Smith and C. Weder, *Adv. Funct. Mater.*, 2001, **11**, 41.

14 S. H. Lee, T. Nakamura and T. Tsutsui, *Org. Lett.*, 2001, **3**, 2005.

15 (*a*) R. C. Ellingson and R. L. Henry, *J. Am. Chem. Soc.*, 1949, **71**, 2798; (*b*) K. Pieterse, J. A. J. M. Vekemans, H. Kooijman, A. J. Spek and E. J. Meijer, *Chem.-Eur. J.*, 2000, **6**, 4597.

16 F. Ogura, Y. Hama, Y. Aso and T. Otsubo, *Synth. Met.*, 1988, **27**, B295.

17 K. W. Blake and P. G. Sammes, *J. Chem. Soc. C*, 1970, 1070.

18 (*a*) Reviews: K. Sonogashira, in *Comprehensive Organic Synthesis*, ed. B. M. Trost and I. Fleming, Pergamon Press, Oxford, 1991, vol. 3, p. 521; (*b*) K. Sonogashira, *J. Organomet. Chem.*, 2002, **653**, 46.

19 D. E. Ames, D. Bull and C. Takunda, *Synthesis*, 1981, 364.

20 Single crystal X-ray diffraction data for compound **12** are from T. B. Marder (private communication).

21 Y. Cao, I. D. Parker, G. Yu, C. Zhang and A. J. Heeger, *Nature (London)*, 1999, **397**, 414.

22 (*a*) P. Cea, Y. Hua, C. Pearson, C. Wang, M. R. Bryce, M. C. López and M. C. Petty, *Mater. Sci. Eng., C*, 2002, **22**, 87; (*b*) P. Cea, Y. Hua, C. Pearson, C. Wang, M. R. Bryce, F. M. Royo and M. C. Petty, *Thin Solid Films*, 2002, **408**, 275.

23 M. J. Frisch, G. W. Trucks, H. B. Schlegel, G. E. Scuseria, M. A. Robb, J. R. Cheeseman, V. G. Zakrzewski, J. A. Montgomery, Jr., R. E. Stratmann, J. C. Burant, S. Dapprich, J. M. Millam, A. D. Daniels, K. N. Kudin, M. C. Strain, O. Farkas, J. Tomasi, V. Barone, M. Cossi, R. Cammi, B. Mennucci, C. Pomelli, C. Adamo, S. Clifford, J. Ochterski, G. A. Petersson, P. Y. Ayala, Q. Cui, K. Morokuma, D. K. Malick, A. D. Rabuck, K. Raghavachari, J. B. Foresman, J. Cioslowski, J. V. Ortiz, A. G. Baboul, B. B. Stefanov, G. Liu, A. Liashenko, P. Piskorz, I. Komaromi, R. Gomperts, R. L. Martin, D. J. Fox, T. Keith, M. A. Al-Laham, C. Y. Peng, A. Nanayakkara, M. Challacombe, P. M. W. Gill, B. G. Johnson, W. Chen, M. W. Wong, J. L. Andres, C. Gonzalez, M. Head-Gordon, E. S. Replogle and J. A. Pople, *GAUSSIAN 98 (Revision A.9)*, Gaussian, Inc., Pittsburgh, PA, 1998.

24 A. D. Becke, *Phys. Rev. A*, 1988, **38**, 3098; A. D. Becke, *J. Chem. Phys.*, 1993, **98**, 5648.

25 C. Lee, W. Yang and R. G. Parr, *Phys. Rev. B*, 1988, **37**, 785.

26 (*a*) P. Flükiger, H. P. Lüthi, S. Portmann and J. Weber, *Molekel, Version 4.2*, Swiss Center for Scientific Computing, Manno, Switzerland), 2000 (http://www.cscs.ch/molekel/); (*b*) S. Portmann and H. P. Lüthi, *Chimia*, 2000, **54**, 766.